THE JOURNAL OF NAVIGATION (2006), **59**, 119–133. © The Royal Institute of Navigation
doi:10.1017/S0373463305003498 Printed in the United Kingdom

Flight Test of Attitude Determination System using Multiple GPS Antennae

Jaegyu Jang and Changdon Kee

(*School of Mechanical and Aerospace Engineering*, *Seoul National University*)
(Email: zang@snu.ac.kr)

Small Unmanned Aerial Vehicles (UAVs) or inexpensive airplanes, such as a Cessna single engine aircraft, require a navigation system with a cheap, compact and precise sensor. Over the past ten years, GPS receivers have begun to be used as primary or alternative navigation sensors, because their use can significantly reduce the overall system cost. This paper describes a navigation system incorporating a velocity-based attitude estimation system with an attitude determination system using multiple antennae, which was implemented and tested using a UAV. The main objective was to obtain precise attitude information using low cost GPS OEM boards and antennae. Attitude boundaries are derived from the relationship between the body frame and the wind coordinates, which are used to validate the resolved cycle ambiguity in an Euler angle domain. Angular rate based on Doppler measurements was used to exclude the degenerate pseudo-roll angle information during severe uncoordinated flight. Searching for cycle ambiguity at every epoch of the flight showed that the developed system gave reliable cycle integer solutions, although the carrier phase measurement was subject to additional errors, such as multipath, external interference, and phase centre variation. A flight test was performed using a 1/4-scale Piper J3 Cub model, CMC Allstar OEM boards, OEM AT575-70 antennae, and 700 MHz PC104 board.

KEY WORDS

1. Attitude Determination. 2. UAV. 3. Ambiguity Resolution. 4. GPS Antennae.

1. INTRODUCTION. Most commercial airplanes use very expensive inertial navigation sensors to ensure safety. However, these are not popular for small and expendable Unmanned Aerial Vehicles (UAVs) or inexpensive aircraft. Therefore, over the past 10 years, attitude determination systems using multiple GPS antennae have been investigated because of their accuracy and cost effectiveness. We can divide these systems into two classes. The first is the dynamic or rotation-based method (Cohen, 1992), which can be used to initialize the cycle ambiguity whilst taxiing on the runway. Because it is difficult to detect and recover small cycle slip (less than 10 cycles) using an inexpensive L1 GPS receiver (Wei et al, 1992), this method is not suitable as an on-the-fly algorithm. The second method is the ambiguity resolution method based on a least squares technique and stochastic verification (Hatch, 1990; Erickson, 1992). However, most research into this method

used relatively expensive GPS receivers to produce accurate and reliable solutions. Recent research showed that the resolved cycle ambiguity using carrier phase measurements from a low cost GPS receiver can be incorrect (Wang et al, 2004). This is the most common and serious problem in the presence of severe multipath or low visibility, particularly in the epoch-by-epoch algorithm, which is generally used for the single frequency GPS (L1) receiver. The problem is caused by selecting a local minimum as the solution. The only practical way to avoid this is to increase the number of antennae as much as possible for a given visibility; however, this means an overall cost increase for the navigation system.

There is another attitude estimation system based on velocity measurements from a single GPS antenna (Kornfeld, 1999). It assumes the coordinated flight conditions of commercial aircraft and uses the wind coordinates for attitude, so its solution has a time varying bias to the traditional body frame coordinates. Although recent research shows it is possible to achieve guidance and control of an aircraft in real-time (Lee et al, 2003; Hsiao et al, 2003), the system is vulnerable as it is significantly dependent upon the vehicle dynamic. Uncoordinated flight during a skidding and slipping turn, yawing manoeuvre or a wind gust induces overshoot, time lag, and other significant biases.

The angular difference between the two coordinate systems is ideally due to two parameters: angle of attack and side slip angle. This paper focuses on rejection of the incorrect cycle ambiguity using boundaries in the Euler angle domain, which was defined by the relationships between the coordinate frames for the given maximum parameters. To produce a reliable boundary we used a kinematic Kalman filter using a pseudo-roll angle based on the velocity vector and rolling rate. For ambiguity resolution, the SNUGLAD (Seoul National University GPS Lab Attitude Determination) algorithm (Kee et al, 2003) was used with three Allstar GPS OEM boards and antennae from CMC electronics. Pseudo-attitude was estimated using acceleration estimated by a Kalman filter on the velocity vector. Results show precise attitude can be determined with single epoch carrier phase measurements from low cost GPS OEM boards and antennae during severe uncoordinated flight conditions of small UAVs.

2. ATTITUDE BOUNDARY.

In contrast to traditional attitude from multiple GPS antennae, which is referenced to the aircraft body axes, wind-axes attitude is referenced to the aircraft velocity vector $\mathbf{v_a}$.. The coordinate frames of the two systems are related through the angle of attack, α, and sideslip angle, β, as shown conceptually in Figure 1. The subscript W denotes the wind frame and b the body frame.

The relationships between Euler angles of the body and the wind coordinates are:

$$R(\psi, \theta, \phi) = R(-\beta, \alpha, o) \cdot R(\psi_W, \theta_W, \phi_W) \tag{1}$$

Useful first order equations can be derived from the above relationship, which means the Euler angle differences between each frame are:

$$sin(\phi - \phi_W) \approx tan\theta_W(\alpha sin\phi_W - \beta cos\phi_W) \tag{2}$$

$$\theta - \theta_W \approx \alpha cos\phi_W + \beta sin\phi_W \tag{3}$$

https://doi.org/10.1017/S0373463305003498 Published online by Cambridge University Press

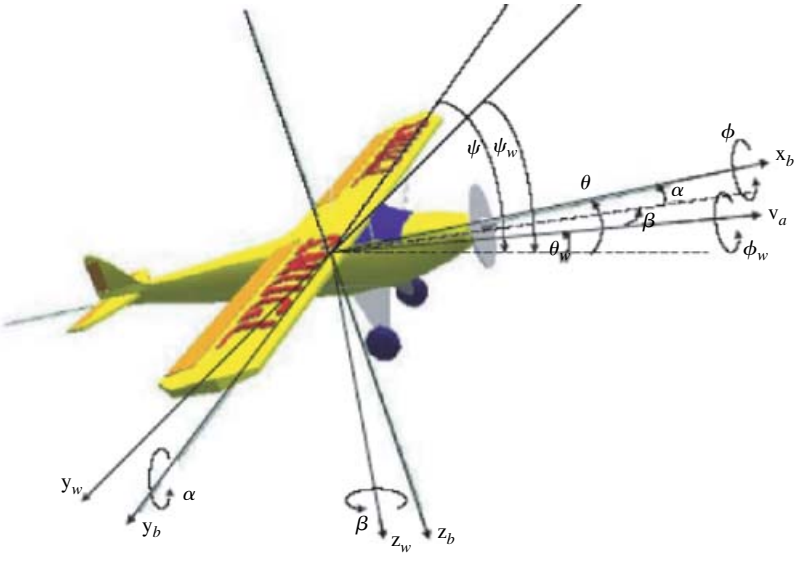

Figure 1. Definition of Euler angles in body and wind coordinates.

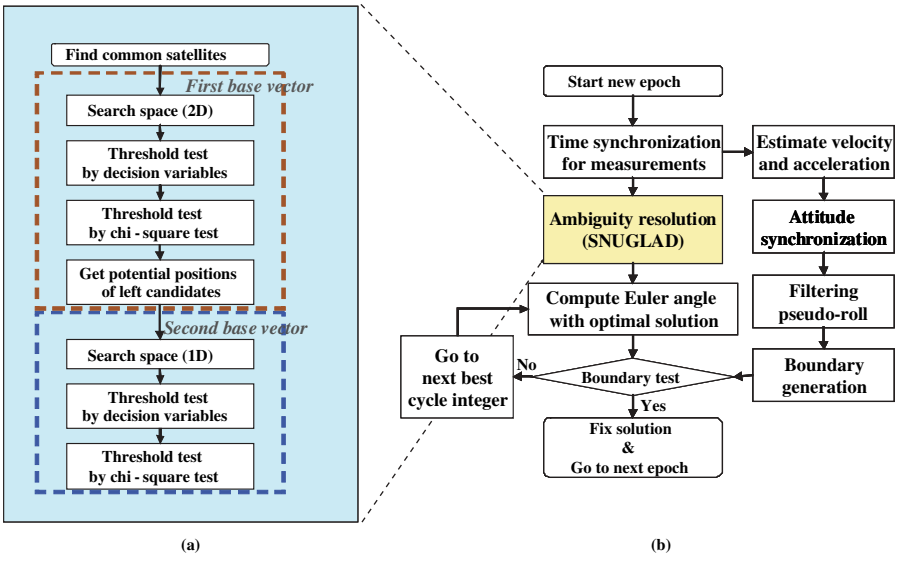

Figure 2. Flow charts. (a) Ambiguity resolution algorithm SNUGLAD; and (b) Overall attitude determination system for flight test.

$$sin(\psi - \psi_W) \approx \frac{\alpha sin\phi_W - \beta cos\phi_W}{cos\theta} \tag{4}$$

In terms of traditional attitude, which is referenced to the body frame, these differences can be understood as an error in the Euler angle domain. In coordinated flight, which is valid for most flight conditions encountered by conventional aircraft,

https://doi.org/10.1017/S0373463305003498 Published online by Cambridge University Press

major errors are caused by the angle of attack in equations 2–4. Overshoot, time lag from Kalman filter estimate and noise in velocity measurement can be treated as additional error sources. With estimated wind-axes attitude called a pseudo-attitude and given maximum values $\alpha_{\max}$ and $\beta_{\max}$, we can define boundaries for the differences. If resolved cycle ambiguity is true, the differences satisfy the boundaries that are defined in equations 5–7. That means we can use the boundaries as a verification area in which the Euler angles derived from resolved cycle ambiguities have to be located.

$$|\Delta\phi| \leqslant tan\tilde{\theta}_W\left(\alpha_{max}\cdot\left|sin\tilde{\phi}_W\right| + \beta_{max}\cdot cos\tilde{\phi}_W\right) + \left|\phi_W - \tilde{\phi}_W\right|_{max} + \sigma_\phi \tag{5}$$

$$|\Delta\theta| \leqslant \alpha_{max}\cdot cos\tilde{\phi}_W + \beta_{max}\cdot\left|sin\tilde{\phi}_W\right| + \sigma_\theta \tag{6}$$

$$|\Delta\psi| \leqslant \frac{\alpha_{max}\cdot\left|sin\tilde{\phi}_W\right| + \beta_{max}\cdot cos\tilde{\phi}_W}{cos\tilde{\theta}_W} + \sigma_\psi \tag{7}$$

where Δ denotes the difference between the pseudo-attitude and the actual attitude. In equation 7, we use the flight path angle $\tilde{\theta}_W$ instead of pitch angle θ because we do not know the correct cycle integers. The maximum angle of attack $\alpha_{\max}$ and sideslip angle $\beta_{\max}$ are defined as positive constants. $\sigma_{(*)}$ includes the attitude noises of the estimates. Velocity and acceleration from the GPS receiver are estimated with reference to the ground instead of the wind coordinates. Therefore, we should consider the difference between wind-axes roll and pseudo-roll, which is the estimated wind-axis roll. It appears as $\left|\phi_W - \tilde{\phi}_W\right|$ in equation 5.

3. UNCOORDINATED FLIGHT & ATMOSPHERIC NON-UNIFORMITIES.

Basically, attitude estimation using the craft's trajectory assumes coordinated flight and uniform wind motion (Kornfeld, 1999), as shown in equation 8:

$$\beta \approx 0,\ \frac{dw}{dt} \approx 0 \tag{8}$$

Where **w** is wind velocity. However, we have to consider the effects of uncoordinated flight, such as during a severe slip, yaw manoeuvre, or during stall, and effects due to atmospheric non-uniformities, such as turbulence or wind shear. In particular light, slow and small aircraft are readily subjected to these conditions. In these cases, true cycle ambiguity can be rejected by the boundaries. The sideslipping and yawing may cause instantaneous or constant offsets, and non-uniformities may cause time varying offsets, overshoot or time lag. We can avoid missing true cycle ambiguity simply by increasing a design parameter, such as maximum sideslip angle and $\left|\phi_W - \tilde{\phi}_W\right|$ in equation 5. However, the worst case may occur in the pseudo-roll angle when lift decreases rapidly, such as in the non-linear flight regime. In this case, the pseudo-roll estimate can be abnormal due to the cancellation between gravity and acceleration. Fortunately, we can estimate an approximate angular rate using Doppler measurements from multiple GPS antennae and the pseudo-attitude matrix $C^n_{b,k-1}$ of the previous period. The rate of attitude matrix, $C^n_{b,k}$ can be calculated using

https://doi.org/10.1017/S0373463305003498 Published online by Cambridge University Press

equation 9:

$$C_{b.k}^{n} = (H^T H)^{-1} H^T \Phi_k (X_b^T X_b)^{-1} X_b^T \tag{9}$$

where H is the single differential line of sight vector of visible GPS satellites, Φ_k is the Doppler measurements from multiple GPS antennae, and X_b is the base vectors of multiple GPS antennae in body coordinates. Abnormal estimation of pseudo-roll is prevented effectively using a Kalman filter with state $X = [\phi \ \dot{\phi} \ \ddot{\phi} \ \dddot{\phi}]^T$. The corresponding process noise covariance matrix, Qk, is determined by the van Loan method (van Loan, 1978):

$$Q_k = \begin{bmatrix} \Delta t^7/252 & \Delta t^6/72 & \Delta t^5/30 & \Delta t^4/24 \\ \Delta t^6/72 & \Delta t^5/20 & \Delta t^4/8 & \Delta t^3/6 \\ \Delta t^5/30 & \Delta t^4/8 & \Delta t^3/3 & \Delta t^2/2 \\ \Delta t^4/24 & \Delta t^3/6 & \Delta t^2/2 & \Delta t \end{bmatrix} S_\phi \tag{10}$$

where Δt is the sampling time and S_ϕ is the white noise spectrum amplitude.

4. SNUGLAD ALGORITHM. Whereas estimates of the position, velocity, and attitude boundaries for the aircraft are performed with a single GPS antenna system, the SNUGLAD algorithm was used for ambiguity searching with multiple GPS antennae, which is designed to reduce the overall computational load for ambiguity searching (Kee et al, 2003). In this section, just the basic concept is introduced to assist in understanding the overall system. Each base vector is searched sequentially for cycle ambiguity as shown in Figure 2(a).

First, potential base vectors on the sphere with a radius of the first base vector are searched in 2D space, and then potential second base vectors are searched in 1D space using the geometric relationships between the base vectors. The decision variables in Figure 2(a) mean noise components of cycle integers about secondary satellite set, which is defined to reject incorrect solutions with the least computation. We did not use a ratio test using the f-distribution because we performed the flight test epoch-by-epoch. The possibility of passing the ratio test using single epoch measurements from a low cost L1 GPS receiver is low, especially when there is multipath, phase centre variation or RF interference; instead, we used the boundary test illustrated in Figure 2(b), which shows the flowchart of the overall system designed for the evaluation flight. Boundaries computed by pseudo-attitude have the role of a verification test for the estimated cycle ambiguity in the Euler angle domain.

5. SYSTEM CONFIGURATION. The UAV used for the flight test was a 1/4 scale Piper J3 Cub, which is a conventional high wing airplane. Three OEM AT575-70 GPS antennae were mounted on the top and a ground plane, made of copper tape, was used to prevent multipath reception during landing or take off. The GPS antenna for estimating velocity is mounted near the centre of gravity to reduce the antenna lever arm motion during pitching (Lee, 2003). Figure 3 shows the 1/4 scale Piper J3 Cup model used for the flight experiment. The designed

https://doi.org/10.1017/S0373463305003498 Published online by Cambridge University Press

Figure 3. 1/4 scale Piper J3 Cub.

lengths of base vectors are 0·5 m and 0·94 m, respectively, which can differ with slight differences between antenna phase centres.

As a low cost navigation sensor, three CMC Allstar OEM boards were used. Each is a 12-channel L1 receiver that can output 10 Hz code and carrier phase measurements through a RS232 port. The PC104 board assembly with a 700 MHz clock was used as the navigation computing unit. Position, Velocity, and Timing (PVT) solutions and attitude estimates were sent to the ground monitoring system through a 900 MHz wireless modem. In the flight experiment, RF interferences caused by PC104 and wireless modem were a considerable problem because the UAV was so small. Ambiguity resolution was impossible with conventional RG174 coaxial cable used for the OEM AT575-70 antenna.

Figure 4 shows a monitoring display captured during a real-time experiment made for the purpose of monitoring the status of the UAV and navigation data in real-time. The monitoring program displays a 3D aircraft motion graphic, conventional attitude indicator, vertical history and horizontal trajectory. Final navigation data and status were recorded for analysis, and attitude data for the display were synthesized with the traditional attitude SNUGLAD algorithm-aided with attitude boundaries based on the velocity vector.

6. FLIGHT EXPERIMENT.

The flight was conducted at a model plane airfield in Han River, Seoul, on December 31, 2004. The objective of the flight test was experimental evaluation of the precise attitude determination system using low cost GPS hardware and a small UAV in coordinated and uncoordinated flight.

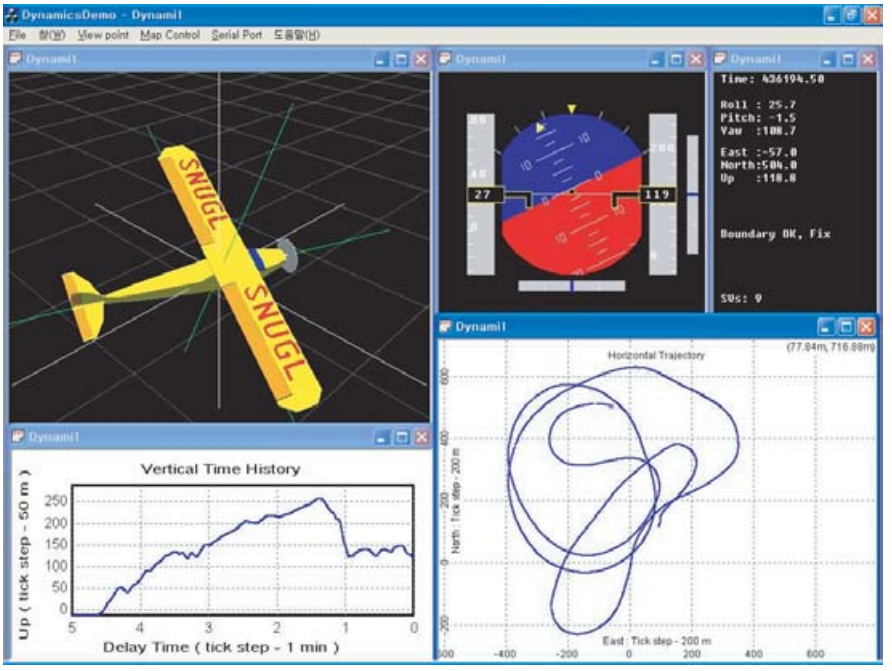

Figure 4. Monitoring display captured during the flight experiment.

This evaluation would show the boundaries which are based on velocity-based attitude with severe offset can verify the resolved cycle ambiguities of the attitude determination system with multiple GPS antennae.

We used three independent GPS OEM boards to determine attitude. This meant the carrier phase measurements from each receiver could have different measured times of one to two epochs due to system delay. In the preprocessing procedure for the system software we used raw measurement buffering and synthesis tasks to synchronize measured time within m seconds. Unfortunately, the CMC Allstar receiver did not output 10 Hz velocity data and Doppler measurements, although they are indispensable for the real-time flight. Therefore, we generated Doppler measurements using the time difference of the raw carrier phase measurements, timed sampling rate, and using cycle slip flag/counter. This method cannot guarantee cycle slip-free measurements. In the experiment, incorrect estimation caused by cycle slip occurred just after touch down, which is outside the scope of this paper. Note that the 10 Hz raw Doppler output option is essential to implement our system perfectly.

Figure 5 shows the ground track during the free flight test for this paper; the figure displays the entire trajectory from take off to landing. It includes climb, descent, shallow and steep turns. The overall flight time was approximately 9 min, and the average speed, except for landing and take off, was approximately 25 m/s; the maximum height above the ground was 247 m.

Soon after take off, the aircraft climbed and turned steeply, which causes typical uncoordinated flight conditions as shown in Figure 6. For 435930–435938 s in GPS

https://doi.org/10.1017/S0373463305003498 Published online by Cambridge University Press

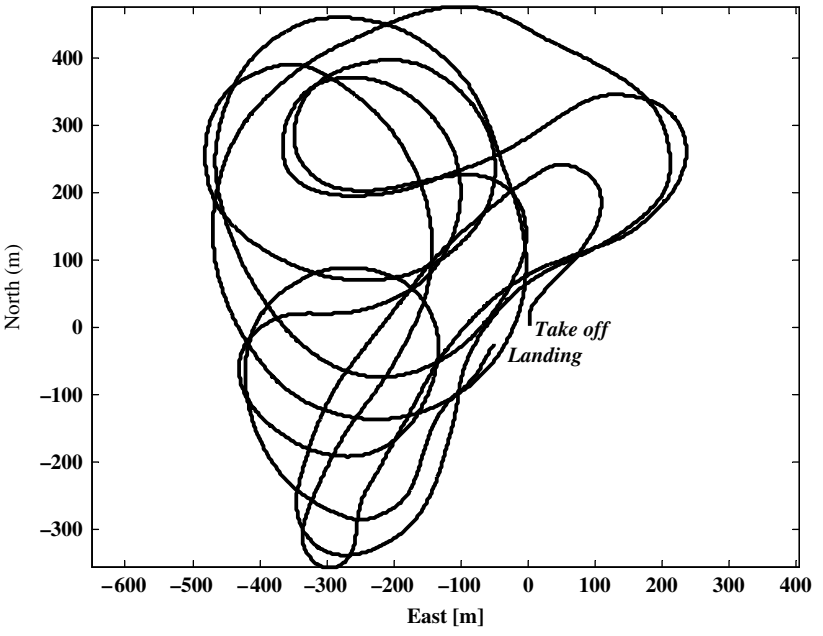

Figure 5. Ground track during flight test (ENU coordinate).

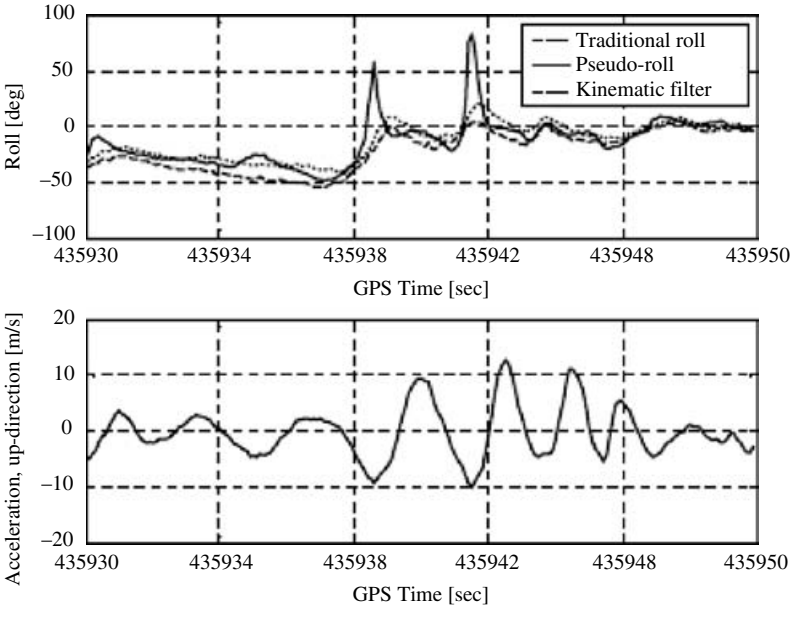

Figure 6. Effects of uncoordinated flight in pseudo-roll.

time, it turned to the left with a roll angle of 27–56°. Maximum 24° offset occurred in the pseudo-roll, which is natural because it experienced a skidding turn. However, for 4 s from 435 938 s, the pseudo-roll shows abnormal estimation results, because

https://doi.org/10.1017/S0373463305003498 Published online by Cambridge University Press

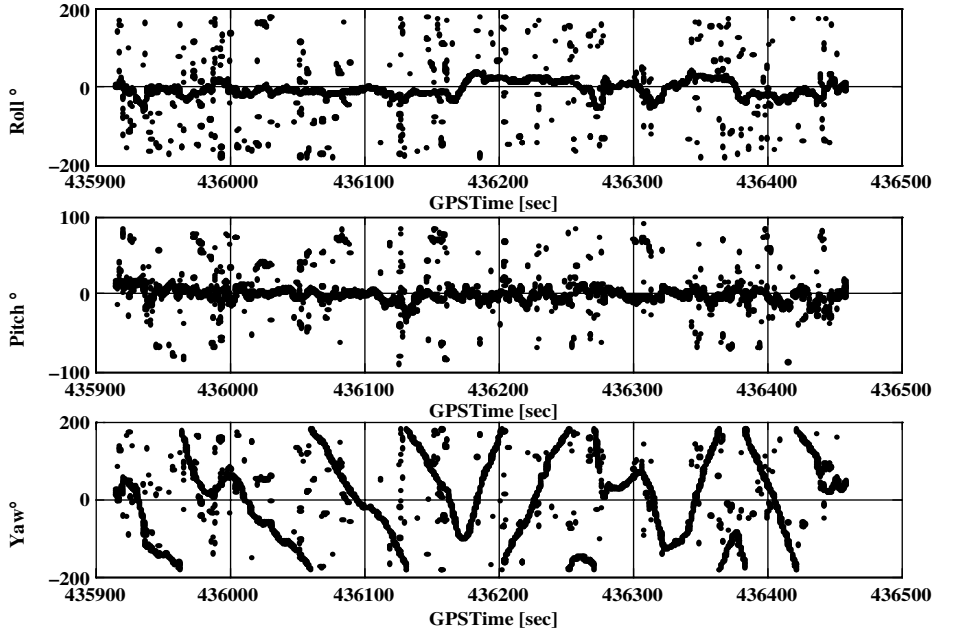

Figure 7. Determined Euler angles by ambiguity searching (w/o ratio test, single epoch measurements were used with a sampling rate of 10 Hz).

the aircraft was in a similar situation to zero gravity. The second graph of Figure 6 shows the acceleration estimate from the Kalman filter in the up-direction of ENU coordinates. During abnormal estimation, the acceleration peak even approached gravity acceleration g. As described in section 3, if lift decreases rapidly, pseudo-roll information degenerates (Kornfeld, 1999). However, we could estimate reasonable pseudo-roll angle from the kinematic Kalman filter described in section 3. In this paper, the difference between pseudo-attitude and traditional attitude by resolved cycle ambiguity is used for boundary check; therefore it is a very important procedure.

We conducted ambiguity resolution with single epoch measurements, firstly to demonstrate the possibility of determining attitude at any time on-the-fly, and secondly because the epoch-by-epoch algorithm is a good way to avoid cycle slip, which is difficult to detect and repair using only a low cost L1 GPS receiver. As a result of ground testing we decided not to use a ratio test in the epoch-by-epoch experiment because the ratio passing rate was too low.

Figure 7 shows the Euler angles determined with a single epoch data from multiple GPS antennae. The number of common satellites was six to seven during the flight experiment with a mask angle of 25°. Figure 7 shows determined attitude by ambiguity resolution only, of which success rate is relatively low as 86%. Ambiguity searching algorithms, such as SNUGLAD, are based on a least squares technique to determine the optimal solution. Generally, the variance factor is used as the objective function and the cycle ambiguity candidate with the minimum variance factor is chosen as the solution (Erickson, 1992). However, in the epoch-by-epoch

https://doi.org/10.1017/S0373463305003498 Published online by Cambridge University Press

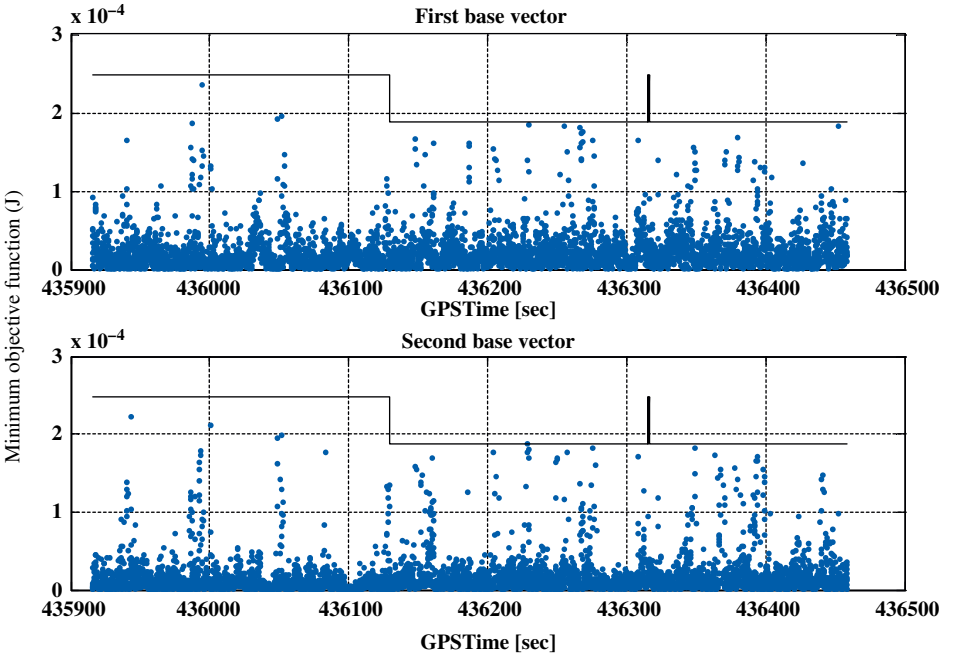

Figure 8. Minimum objective functions of master and secondary base vectors. Confidence level for Chi-square test is 99·99%.

algorithm, there is a relatively high probability of choosing a local minimum as the solution instead of the global minimum because there is no way to distinguish a local minimum from the global minimum using conventional ambiguity resolution algorithms.

Figure 8 shows the minimum objective functions, which are the smallest variance factors. We can consider the reasons for the fluctuations in Figure and low success rate in Figure 7 as follows: multipath from ground plane or avionics box, RF interference from the PC104 and wireless modem, and GPS antenna phase centre variations. Of these, RF interference appears to be the largest error source; more careful shielding and grounding may be helpful in reducing the interference. The antenna's phase centre is not a physically fixed point; it changes with the direction of the incoming signals, and recent research shows it can vary up to 10 cm vertically (Wang, 2003). Antenna phase centre variations can be reduced by careful antenna alignment and estimation using mapping (Gebre-Egziabher et al, 1998).

We defined the attitude boundaries in section 2 to check and reject incorrect cycle ambiguity. Figure 9 shows the boundaries and estimated errors. If the estimated errors satisfy the defined boundaries simultaneously, we show them in the illustration as a solid line instead of a dot. The maximum angle of attack, $\alpha_{\mu\alpha\xi}$ is defined as 10° and sideslip angle $\beta_{\mu\alpha\xi}$ as 10°. In moderate gust conditions, we can define $\beta_{\mu\alpha\xi}$ as 5° (3σ) for the aircraft with 25 m/s nominal speed (Bryson, 1994). However, we assumed a side gust velocity of 1·4 m/s because we had to consider

https://doi.org/10.1017/S0373463305003498 Published online by Cambridge University Press

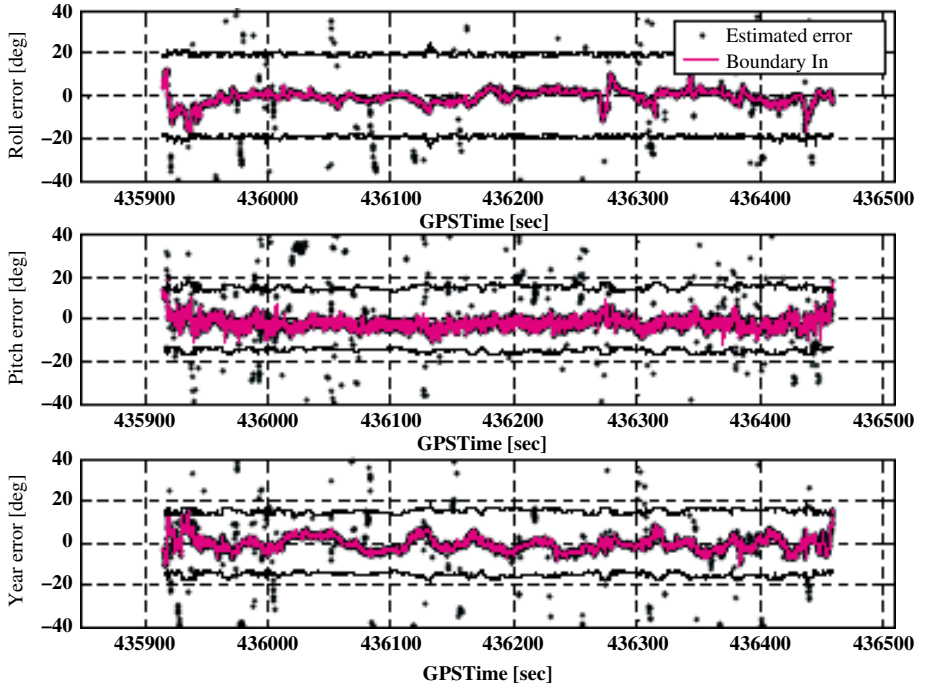

Figure 9. Attitude boundaries and errors, the Euler difference between the frames using estimated cycle ambiguity and pseudo-attitude. 'Boundary In' means the errors satisfy all boundaries simultaneously.

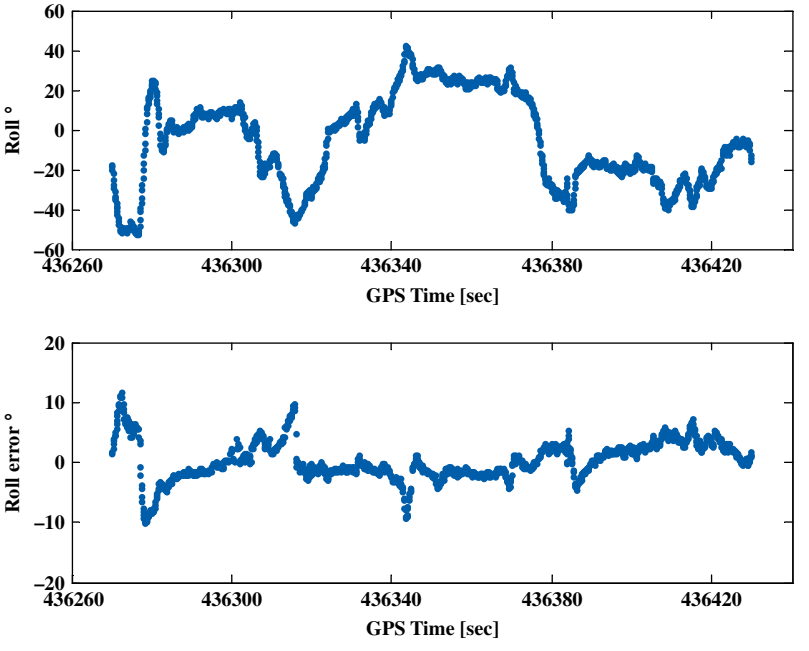

Figure 10. Roll angle and roll error: the estimated difference between the coordinate frames.

https://doi.org/10.1017/S0373463305003498 Published online by Cambridge University Press

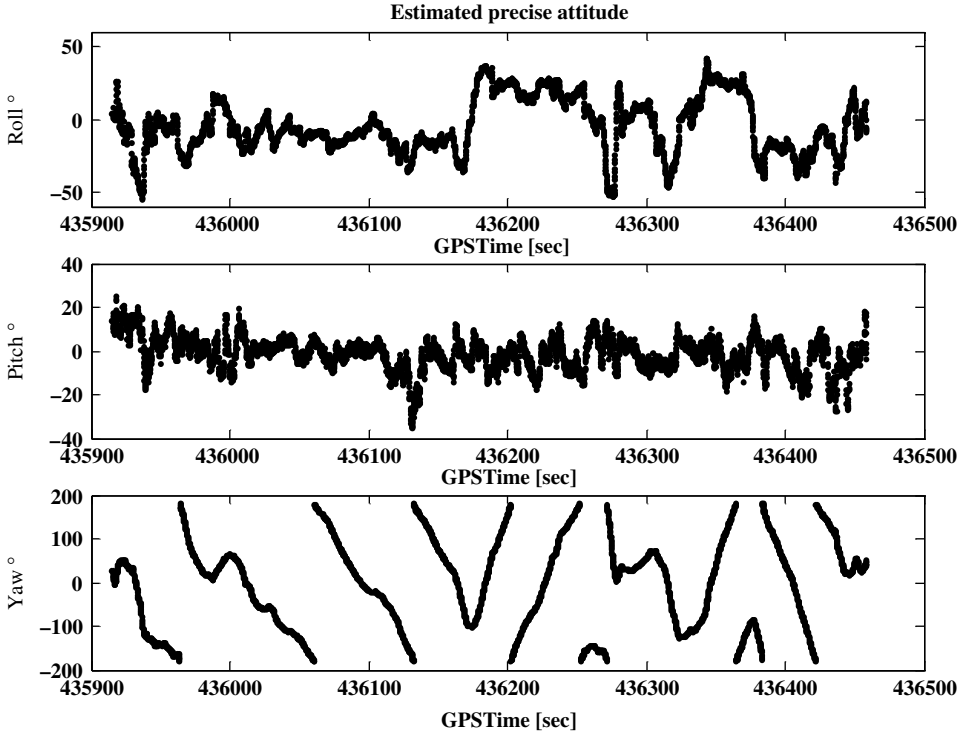

Figure 11. Traditional attitude determined by SNUGLAD aided by velocity-based boundaries.

severe uncoordinated flight. Because the velocity with reference to the ground is used with GPS Doppler measurements, the pseudo-roll, $\tilde{\theta}_W$ may be different to the theoretical wind-axes roll, θ_W (Kornfeld, 1999). This difference, $|\phi_W - \tilde{\phi}_W|_{max}$, was assumed to be 15° in the flight experiment. During steep turns or rapid roll motion, the difference may increase considerably. In Figure 10, the roll angle and the error, which is the difference between roll and pseudo-roll, are illustrated between 436270 and 436320 s. This shows that the error is correlated with roll angle. Therefore, we deduce that the constant $|\phi_W - \tilde{\phi}_W|_{max}$ should be defined based on the dynamics of the aircraft.

Figure 11 shows the Euler angles determined using SNUGLAD aided by the attitude boundaries defined in section 2. While in Figure 7 incorrect cycle ambiguities were determined as solutions at a rate of approximately 14% using real-time ambiguity resolution, incorrect cycle ambiguities were successfully rejected in the Euler angle domain with the suggested system during the flight test. True cycle ambiguities for this analysis were determined from post-processing using Matlab. Because we did not use an additional reference system to analyse the estimated solutions, post-processing used all measurements taken during the flight. Residual check for a given fixed cycle ambiguity was used to check incorrect cycle ambiguity of the real-time attitude determination algorithm for the experiment as well as a geometric check using pseudo-attitude. During post-processing we found some periods did not have real-time solutions, for two reasons. First is the problem of

https://doi.org/10.1017/S0373463305003498 Published online by Cambridge University Press

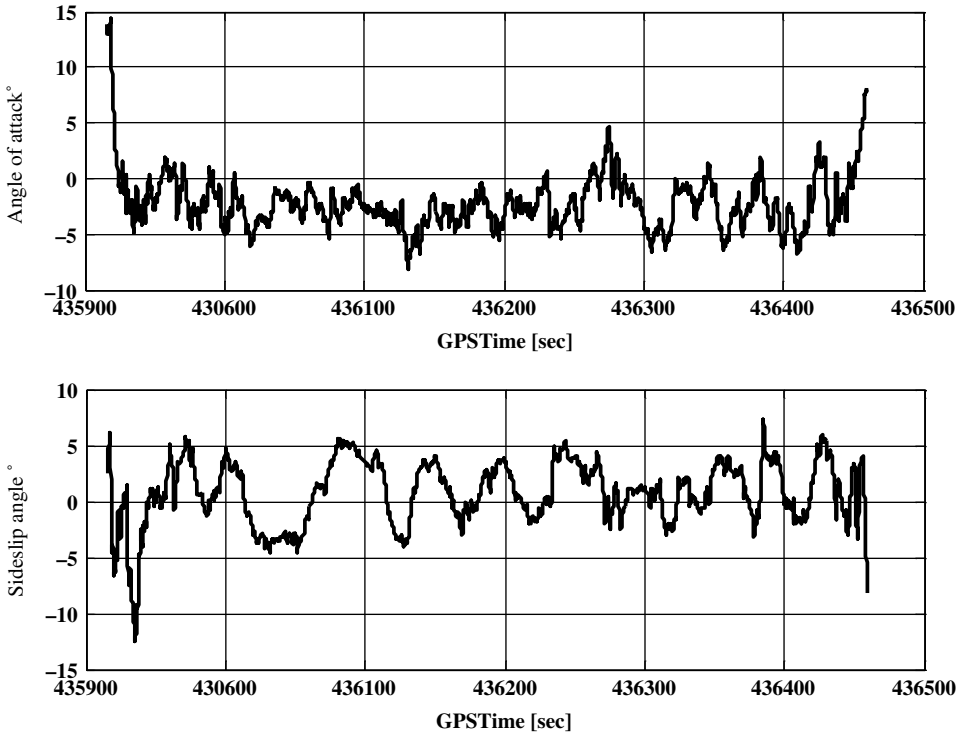

Figure 12. Angle of attack and sideslip angle estimates.

time synthesis for measurements from each CMC Allstar receiver, which caused a system delay, such as data communication using RS232 ports or a raw data parsing procedure. These are simply a data management issue, so there is no problem in post-processing for data analysis. The second problem is caused during the residual check procedure, which uses the chi-square distribution. Figure 8 shows the residuals have coloured noise components; sometimes the residual may not satisfy the threshold, which means true cycle ambiguities were rejected during the flight test. In the static test, which was conducted before the flight test, double difference residuals were up to almost 4 cm, and recent research (Wang et al, 2004) shows the residuals reach up to 7–8 cm even if the cycle ambiguities are correctly determined. This means it can be impossible to resolve correct solutions. However, the solution can be estimated using Doppler measurements if there are no small cycle slips (0·5 or 1 cycle). As described above, offset in the residuals is due to RF interference, multipath or antenna phase centre variations. Low cost GPS antennae and coaxial cable are more vulnerable to these error sources. This may cause large attitude errors to some degree for a short baseline or can make ambiguity resolution difficult.

The speed limit to enable the employment of velocity based attitude was defined as 3 m/s in the flight experiment using the 1/4 size Piper J3 Cub. The airplane took off at a speed of 9–10 m/s and landed at 8–9 m/s. Therefore Figure 11 includes almost all the flight mission from take off to landing. This means that

https://doi.org/10.1017/S0373463305003498 Published online by Cambridge University Press

SNUGLAD aided by velocity based attitude can be used during landing or take off with low velocity as well as during a high-speed mission. However, it is difficult to use pseudo-roll from touch down to taxiing. In this case possible pitch and roll criteria can be the only reasonable constraint to aid the ambiguity search system.

Contingent on the successful estimation of cycle ambiguity, the angle of attack and sideslip angle can be estimated using equation 11, which is derived from equations 3 and 4:

$$\begin{bmatrix} \tilde{\alpha} \\ \tilde{\beta} \end{bmatrix} = \begin{bmatrix} cos\tilde{\phi}_W & sin\tilde{\phi}_W \\ sin\tilde{\phi}_W & -cos\tilde{\phi}_W \end{bmatrix}^{-1} \begin{bmatrix} \tilde{\theta} - \tilde{\theta}_W \\ (\tilde{\psi} - \tilde{\psi}_W)cos\tilde{\theta} \end{bmatrix} \tag{11}$$

While sideslip and angle of attack should be estimated using a velocity vector with respect to the air, we used velocity with respect to the ground. Therefore, the accuracy is dependent on the aircraft dynamics and the surrounding wind conditions. Figure 12 shows the estimated angle of attack and sideslip angle during the flight, which is averaged with a time constant of 1 s. For approximately the first 430600 s the aircraft was climbing and making steep turns and then finally descending with steep turns. Figure 12 shows the correct tendency to some degree because α and β have close correlation with lift or speed and side force. We believe that although a result using equation 11 cannot guarantee accurate estimation it will be useful information for the aircraft in moderate coordinated flight motion.

7. CONCLUSIONS. We conducted flight testing using a 1/4 size Piper J3 Cub to evaluate the performance improvement of attitude determination system by combining multiple GPS antennae and a single GPS antenna. Pseudo-attitude with offset error was used to make attitude boundaries, which are derived from the relationship between the body coordinates and the wind coordinates. Resolved cycle ambiguities were checked using boundaries in the Euler angle domain as a verification test. Problems during uncoordinated flight conditions were encountered and pseudo-roll was filtered using Doppler measurements to overcome the degeneration of roll angle information during the non-linear flight regime. The free flight test, including uncoordinated flight, was conducted with low cost receivers and antennae. Although GPS measurements were plagued with RF interference, from the PC104 and modem or due to antenna phase centre variations, the experimental results showed incorrect cycle ambiguities were effectively rejected by the boundaries.

REFERENCES

Bryson, E. Jr (1994). *Control of Spacecraft and Aircraft*. Princeton University Press.

Cohen, C.E. (1992). *Attitude Determination Using GPS*. Ph.D. thesis, Stanford University.

Erickson, C. (1992). *Investigations of C/A Code and Carrier Measurements and Techniques for Rapid Static GPS Surveys*. M.Sc. thesis, University of Calgary.

Gebre-Egziabher, D, Hayward, R.C. and Powell, J.D. (1998). A Low-Cost GPS/Inertial Attitude Heading Reference System (AHRS) for General Aviation Applications. *1998 IEEE Position, Location and Navigation Symposium — PLANS '98*, Palm Springs, California, April.

Hatch, R. (1990). Instantaneous Ambiguity Resolution. Proceedings of the IAG International Symposium 107 on Kinematic Systems in Geodesy, Surveying and Remote Sensing, Banff, Canada, September, 1990, Springer-Verlag, New York, pp. 299–308.

Hsiao, F., Huang, S. and Lee, M. (2003). The study of real-timed GPS navigation accuracy during approach and landing of an ultralight vehicle. *Proceedings of International Conference on Recent Advances in Space Technologies, 2003. RAST '03*, IEEE, Istanbul, Turkey.

Kee, C., Jang, J. and Sohn, Y. (2003). Efficient Attitude Determination Algorithm using Geometrical Concept: SNUGLAD. *2003 National Technical Meeting Proceedings, Anaheim, California*, January 22–24.

Kornfeld, R.P. (1999). *The Impact of GPS Velocity Based Flight Control on Flight Instrumentation Architecture*. Ph.D. thesis, Massachusetts Institute of Technology.

Lee, S., Lee, T., Park, S. and Kee, C. (2003). Flight Test Results of UAV Automatic Control Using a Single-Antenna GPS Receiver, *AIAA GN&C Conference and Exhibit*, 2003, AIAA-2003–5593.

Van Loan, C.F. (1978). Computing Integrals Involving Matrix Exponential, *Transactions on Automatic Control, IEEE*. vol. ac-23, no. 3, June.

Wang, C. (2003). *Development of a Low-cost GPS based Attitude Determination System*. M.Sc. thesis, Department of Geometrics Engineering Report No. 20175, University of Calgary.

Wang, C., Lachapelle, G. and Cannon, M.E. (2004). Development of an Integrated Low-Cost GPS/Rate Gyro System for Attitude Determination. *Journal of Navigation*, **57**, 85–101.

Wei, M., Cannon, M.E. and Schwarz, K.P. (1992). Maintaining high accuracy GPS positioning 'on the fly'. *Proceedings of PLANS'92*, Monterey, March 25–27, IEEE, New York.